sustainability

MDPI

Article

The Impact of Land Use/Cover Change on Ecological Environment Quality and Its Spatial Spillover Effect under the Coupling Effect of Urban Expansion and Open-Pit Mining Activities

Haobei Liu †, Qi Wang †, Na Liu *, Hengrui Zhang, Yifei Tan and Zhe Zhang

School of Surveying and Geo-Informatics, Shandong Jianzhu University, Jinan 250101, China; 202016104063@stu.sdjzu.edu.cn (H.L.); wangqi19@sdjzu.edu.cn (Q.W.); 202016104048@stu.sdjzu.edu.cn (H.Z.); 202116104004@stu.sdjzu.edu.cn (Y.T.); 2022165115@stu.sdjzu.edu.cn (Z.Z.)
* Correspondence: liuna20@sdjzu.edu.cn
† These authors contributed equally to this work.

Abstract: Suburban open-pit mining concentration areas are both the frontline of urban expansion and the main battlefield in mineral resource development. These dual forces have resulted in significant land use/cover changes (LUCC), which play a crucial role in determining the ecological environment quality (EEQ). However, research examining how LUCC affects EEQ under the coupled impact of these two development events is currently lacking. In this study, the response of EEQ to LUCC was evaluated using Landsat images from 2000, 2010, and 2020 for the southern suburban open-pit mining concentration area in Jinan City. A relative contribution index was used to address the ecological and environmental effects of non-dominant land use/cover types, and the impact of LUCC on EEQ and its spatial spillover effects were revealed by also carrying out a buffer zone analysis. The findings of this study indicate that: (1) the dominant land use/cover types that influence the EEQ spatial pattern are farmland, grassland, and construction land. Among them, the area of farmland was the largest, with more than 1800 km^2. Changes in non-dominant land use/cover types to mining land and mine rehabilitation made the most significant relative contribution to the changes in EEQ, i.e., 0.0735 and 0.0184, respectively. (2) The transformation of farmland into construction land and mining land and woodland into mining land was shown to exacerbate the deterioration of the EEQ in the study area, with a deterioration area of 1367.54 km^2 and spatial spillovers of up to 1000 m. (3) Returning farmland to woodland and grassland, as well as returning mine rehabilitation, were found to be the main factors contributing to the improvement of EEQ in the study area, with an improvement area of 1335.67 km^2 and spatial spillover extending from 500 to 800 m. (4) Nevertheless, uneven changes in land use/cover continue to aggravate the agglomerative effect of EEQ deterioration. Further refinement and enhancement of the methods and standards of ecological governance are urgently needed to counterbalance the uneven spatial spillover effects between ecological degradation and improvement. This study provides a scientific reference for the promotion of ecological protection and sustainable development in mining cities.

Keywords: urban expansion; mining and rehabilitation; LUCC; ecological environment quality assessment; RSEI; GeoDetector

check for updates

Citation: Liu, H.; Wang, Q.; Liu, N.; Zhang, H.; Tan, Y.; Zhang, Z. The Impact of Land Use/Cover Change on Ecological Environment Quality and Its Spatial Spillover Effect under the Coupling Effect of Urban Expansion and Open-Pit Mining Activities. *Sustainability* **2023**, *15*, 14900. https://doi.org/10.3390/su152014900

Academic Editors: Yuanzhi Yao, Xiaoai Dai and Zekun Wang

Received: 8 September 2023
Revised: 3 October 2023
Accepted: 11 October 2023
Published: 16 October 2023

1. Introduction

Urban expansion and mineral resource exploitation have facilitated socio-economic development, while also resulting in significant land use/cover changes (LUCC). As a consequence, they have given rise to numerous ecological and environmental issues [1], such as urban heat islands [2], water pollution [3], floods [4], soil erosion [5], biodiversity loss [6], and a decline in ecological environment quality (EEQ) [7]. These problems pose serious threats to ecological security and sustainable development. The processes of urban expansion and mineral resource development need to consider the long-term sustainability of ecosystems, including the preservation of biodiversity and the restoration of ecosystems [8]. This implies the need to implement measures to mitigate ecological damage. Thus, it is crucial to study how LUCC affects the EEQ in urban expansion and resource development settings. Such research endeavors will provide a solid theoretical foundation for the formulation of effective ecological environment protection and management policies [9] and will contribute to the development of sustainable development strategies [10].

The term “suburban open-pit mine concentration area” refers to a complex area where agriculture serves as the primary industry, but where mineral resources are also developed, processed, and utilized within the context of industrialization, urbanization, and urban–rural integration [11]. Despite the relatively small sizes of suburban open-pit mining concentrations, their locations and fragile ecosystems result in strong interactions between human activities and the natural environment, which, in turn, lead to serious ecological and environmental problems. This phenomenon is prevalent globally, in many regions and under different landform types. For instance, regions such as Yakutia [12] in Russia, Jodhpur [13] in India, and Shuozhou [14], Panzhihua [15], and Datong [16] in China have experienced severe ecological degradation due to mineral resource exploitation, resulting in the escalation of ecological and environmental challenges. Therefore, it is imperative to adopt practical and effective measures to attain a harmonious balance among urban development, resource exploitation, and ecological preservation. Nevertheless, compared to other areas, the LUCC in such complex areas is quite complex. The main reason for this is that such areas are unique, consisting of multiple ecological subsystems which face various concurrent development and conservation issues. Key challenges include (1) the prominent conflict between agricultural production and mining development; (2) the concentration of mine pits and associated facilities leading to the occupation and degradation of extensive tracts of ecological lands, such as woodlands and grasslands; and (3) the severe threat to the ecological environment due to rapid urbanization [11,17–19]. In this context, effectively managing the relationship between service functions and the adverse effects of resource extraction is pivotal for the planning and management of concentrated suburban open-pit mining areas [11]. Therefore, for the concentrated mining areas of suburban open-pit mines, it is highly relevant to study the patterns of LUCC and its ecological environmental response mechanism under the coupling effect of urban expansion and mineral resource development for the coordinated development of society, the economy, and ecology in the future [20].

EEQ is a metric for the comprehensive measurement of the elements, structures, and functions of an ecosystem in time and space. It reflects ecological condition under external stress, the viability of human survival, and the potential for sustainable social and economic growth [21]. Currently, two types of quantitative methods are employed for evaluating EEQ [21]. The first type is single factor-based analysis [22], which utilizes parameters such as NPP [23], NDVI [24], LST [21], and TDVI [25]. However, relying on a single parameter or index often fails to capture the overall state of and changes in regional comprehensive EEQ [26]. This is due to the complexity, dynamism, and multifaceted influences of ecological, environmental, and human factors on ecosystems [27]. The second type comprises integrated methods based on multiple factors, such as the ecological environment index (EI) and remote sensing ecological index (RSEI). The EI integrates indicators such as biological richness, vegetation cover, water network density, soil stress, and pollution load [28]. However, this method still faces great challenges due to its dependence on the acquisition of extensive statistical data [29]. In response to the above challenges, Xu [30] proposed the RSEI. This approach enables rapid monitoring and assessments of regional EEQ over a long time period. RSEI is an index based entirely on remotely sensed data, integrating multiple ecological factors. Its advantages lie in the integration of the rationality of EI weights, the setting of normalization coefficients, the accessibility of indicators, and the visualization of ecological environment status [30,31]. Furthermore, RSEI utilizes four ecological and environmental components to reflect the EEQ of a given area and assigns weights to each index using PCA, resulting in highly objective, stable, and visible results [32].

The RSEI has been extensively employed in recent years to assess EEQ in various ecosystems, including urban clusters [33], watersheds [34], mining areas [35], lakes [36], islands [37], and oases [38]. Among these ecosystems, the ecological environments of mining areas exhibit more sensitive and complex biophysical features compared to other areas [39]. In assessments of EEQ in mining areas, many scholars have explored the relationship between RSEI and influencing factors such as urban expansion [40], land use/cover [41], vegetation cover [42], soil quality [43], and temperature change [44]. Moreover, the exploration of relevant drivers has revealed the dominant role of LUCC in shaping EEQ and its impact on the stability of ecosystem structures and functions [45]. However, in the context of suburban open-pit mining concentrations, changes in EEQ are influenced by both urban expansion and activities related to mining and rehabilitation. Currently, there are relatively few studies on how LUCC, under the coupled effects of urban expansion and mining activities, specifically affect changes in EEQ. Therefore, there is an urgent need to explore the mechanisms through which LUCC in suburban open-pit mining concentrations affect changes in EEQ. Such investigations will provide valuable insights into ecological environment protection, as well as land planning and management, within suburban open-pit mining areas.

Given the aforementioned issues, our study focuses on the open-pit mine concentration areas located in the southern mountainous region of Jinan City, Shandong Province, China. The objective of this study is to reveal the mechanisms by which LUCC influenced EEQ under the coupling effect of urban expansion and mine development from 2000 to 2020. The specific targets are: to (1) analyze the characteristics of spatial and temporal changes in land use/cover in the study area during the 2000–2020 period; (2) elucidate the spatial and temporal response patterns of EEQ to LUCC; (3) reveal the extent of the absolute and relative influence of LUCC on EEQ changes, as well as interactions among and the range of their spatial spillovers; and (4) thoroughly examine the relationship between land demand, policy implementation, and LUCC and changes in EEQ. The findings of this study are expected to provide theoretical guidance and decision-making support for the development and rehabilitation of concentrated mining areas in suburban open-pit mines, as well as to promote the sustainable development of the regional ecological environment in the study area.

2. Materials and Methods

2.1. Study Area

The Yellow River Basin holds a crucial and strategic role in China's ecological security, as well as its economic and social development. The Yellow River Basin, serving as China's "energy basin", experienced varying degrees of resource depletion, environmental pollution, and ecological damage due to urban expansion and resource development. Shandong Province, the most economically developed and densely populated region in the Yellow River Basin, has witnessed rapid urban expansion and intense land development Jinan City, which serves as both the center city of the Yellow River Basin and the capital of Shandong Province. These developments have substantially intensified changes in land use and had a significant impact on the local ecology. Jinan City is geographically positioned between 36°01′ and 36°50′ north latitude and between 116°16′ and 117°45′ east longitude (Figure 1a,b), covering an approximate total area of 3270 km^2. The region has a moderate monsoon climate with four distinct seasons and a more pronounced monsoon influence. It has an annual average temperature of 12.8 °C and receives an average annual precipitation of 680 mm.

The southern mountainous area of Jinan City encompasses several administrative regions, including Pingyin County, Changqing District, most of Shizhong District, the central area of Licheng District, and the southern area of Zhangqiu District (Figure 1c). It holds significant importance as a part of Jinan City, at the forefront of urban expansion and intense mining activities, and serves as a crucial ecological protection area due to its abundant water and forest resources. The area is also known for its contribution as a spring-supporting region for Jinan City. To protect the ecological environment of the area, the Jinan government has implemented a series of measures, including strengthening water resources protection, afforestation, and mining remediation. These actions have significantly contributed to the protection of the ecological environment in the southern mountainous area. As a result, it has become a prime example of ecological protection within Jinan City.

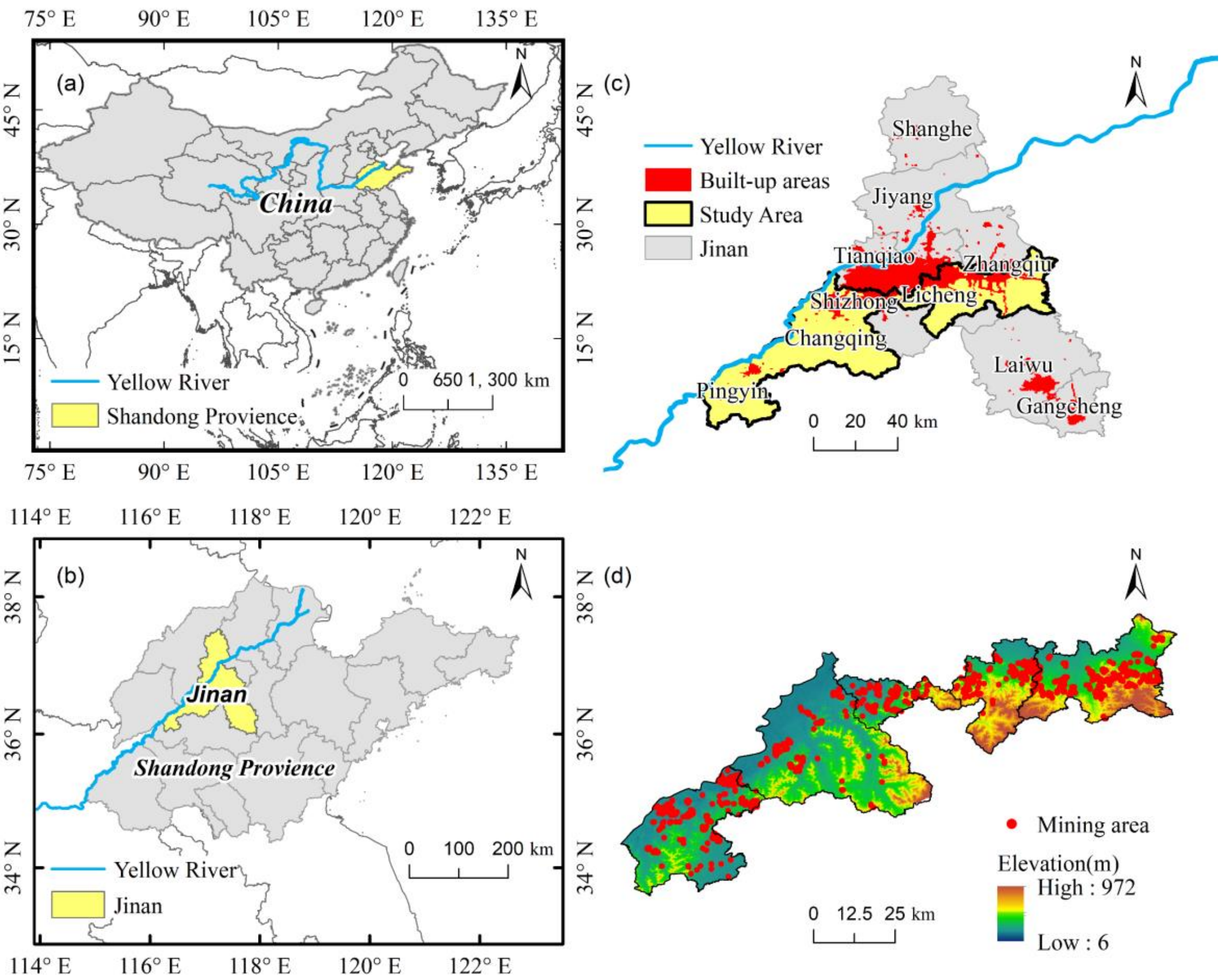

Figure 1. Study area. (**a**) The location of Shandong Province in China, (**b**) the location of Jinan City in Shandong Province, (**c**) the location of the study area in Jinan City and its administrative division, and (**d**) the topography of the study area.

The study area's terrain gradually descent from south to north, comprising low mountains, hills, plains, and abundant mineral resources (Figure 1d). According to the overall planning of mineral resources in Jinan, open-pit mining primarily focuses on non-metallic construction materials such as limestone, granite, and clay used for bricks and tiles. Quarrying in this region often disrupts the local topography and geomorphology, resulting in changes to the natural landscape and the occupation and depletion of extensive land resources. This process seriously undermines environmental stability and sustainability and has significant and far-reaching negative impacts on local ecosystems and land resources. To promote the sustainable development of the area, it is essential to enhance ecological environment protection measures in the southern mountainous area.

2.2. Data Source

This study primarily utilized Landsat satellite image data from the years 2000, 2010, and 2020, which were obtained from the USGS (https://glovis.usgs.gov/ (accessed on 1 October 2022)). For the Landsat7 satellite data loss problem, we use the ENVI5.6 repair plugin landsat_gapfill.sav to repair lost strips. When assessing EEQ, the contribution of forest and other vegetation is of utmost importance. Therefore, image data from July to September, the period of peak vegetation growth, should be used whenever possible. However, it is challenging to obtain high-quality data during this period because it is often accompanied by higher precipitation and cloud-shadow shading. Therefore, we extended the data acquisition time frame from June to October (Table 1) to maximize the available data. The data were pre-processed with radiometric calibration, atmospheric correction, and image stitching after the acquisition, and finally, the study area images were obtained by cropping using the study area boundary vector data.

Table 1. Landsat image data source information.

Year	Sensors	Path	Row	Date	Cloudage
2000	Landsat7 ETM+	122	34	14 September 2000	0.49%
		122	35	14 September 2000	0.15%
2010	Landsat7 ETM+	122	34	28 October 2010	0.00%
		122	35	28 October 2010	0.01%
2020	Landsat8 OLI	122	34	28 August 2010	2.78%
		122	35	28 August 2010	3.90%

After preprocessing, eCognition Developer 9.0 software was employed for land use/cover interpretation. Some of the samples were labeled through visual interpretation using Landsat images and Google Earth, whereas the remaining samples were obtained from field survey data. Subsequently, the study area was classified into eight categories: farmland (FL), woodland (WL), grassland (GL), water area (WA), unused land (UL), construction land (CL), mining land (ML), and mining rehabilitation (MR). The classification was performed using the random forest model-based object-oriented classification method, coupled with visual interpretation. It is worth noting that mine rehabilitation, which is a combination of various types such as woodland, grassland, and farmland formed by the original mining land after rehabilitation, was introduced as a new land use/cover category. After the classification, we conducted visual corrections on the classification results, achieving an overall classification accuracy of 87%, in line with this study's requirements. The land use/cover decoding results will serve as the driving factors for the ensuing changes in EEQ.

2.3. Methods

2.3.1. LUCC Dynamic Analysis

- LUCC transfer matrix

Compared to reflecting static LUCC area data, the LUCC transfer matrix provides a more accurate depiction of the overall trends and structural changes in LUCC over time [46].

$$a_{ij} = \begin{bmatrix} a_{11} & a_{12} & \cdots & a_{1n} \\ a_{21} & a_{22} & \cdots & a_{2n} \\ \cdots & \cdots & \cdots & \cdots \\ a_{n1} & a_{n2} & \cdots & a_{nn} \end{bmatrix} \quad (1)$$

In Equation (1), a represents the area; n is the number of land use/cover types before and after the transfer, i, j $(i, j = 1, 2, \ldots, n)$ represents the land use/cover types before and after the transfer, respectively; a_{ij} represents the area of type i converted to type j before the transfer.

- Single land use/cover dynamic degree

The degree of movement is quantified by measuring the change in the area of a certain land use/cover type within a defined time frame and can be used to study the scale of LUCC occurring within a specific timeframe [47]:

$$R_i = \frac{U_{bi} - U_{ai}}{U_{ai}} \times \frac{1}{T} \times 100 \quad (2)$$

In Equation (2), R_i represents the land dynamic degree of land use/cover type i in the study area; U_{ai} represents that it is the area of land use/cover type i at the beginning of this study, and U_{bi} represents that it is the area of land use/cover type i at the end of this study; T is the length of study time, in years, and this study takes 10 years as the span.

2.3.2. Assessment of EEQ

The assessment of EEQ was conducted using RSEI. RSEI integrates four indicators, namely NDVI, WET, NDBSI, and LST, which represent the factors of vegetation greenness, land moisture, land dryness, and surface temperature, respectively. After normalizing these indicators, PCA was used to synthesize the indicators. The PC1, which contributes more than 80%, has been chosen as the representative measure of the EEQ status within the study area. Because RSEI is primarily used in land-dominated areas, it is not suitable for large water areas. Therefore, we calculated the Normalized Difference Water Index (NDWI) to mask the water bodies in the study area. It is important to emphasize that if the indicators of greenness and humidity, which have a positive impact on EEQ, yield negative values, the calculation results should be adjusted using Equation (3). Additionally, the RSEI values should be normalized (Equation (4)) to facilitate analysis and enable easier comparisons. A higher RSEI value indicates better EEQ in the area, while a lower value indicates lower EEQ. The formulas for calculating the four indicators are shown in Appendix A.

$$RSEI_u = \begin{cases} PC1[f(G,W,T,D)], LV_G, LV_W > 0 \\ 1 - PC1[f(G,W,T,D)], LV_G, LV_W < 0 \end{cases} \quad (3)$$

$$RSEI_v = \frac{RSEI_u - RSEI_{umin}}{RSEI_{umax} - RSEI_{umin}} \quad (4)$$

In Equations (3) and (4), G represents greenness, W represents moisture, T represents heat, D represents dryness, and LV_G, LV_W are greenness and humidity load values. $RSEI_u$ represents the initial ecological index, that is, the image after data fusion is PCA transformed and $PC1$ is calculated, and further transformation is done to ensure that $PC1$ is proportional to the EEQ. $RSEI_v$ represents the normalized $RSEI_u$.

2.3.3. Analysis of the Effects of LUCC on the EEQ

- Quantification of the impact factors' contribution

The quantification of influence factor contributions was performed using GeoDetector's factor detection module, and the results represented by the q value (Equation (5)). This module is designed to identify the key factors influencing geographic phenomena and to evaluate their absolute contributions. In this study, this module was utilized to assess the absolute impact of the different factors X on the spatial variability of the dependent variable Y. Furthermore, for suburban open-pit mining concentrations, although mining land does not constitute the largest land area, mining activities are highly active in these regions. Therefore, to reveal the impact of changes in non-dominant land types on EEQ, we proposed a relative contribution index. This index is founded on the q value acquired through the factor detection, specifically the q value per unit area (Equation (6)).

$$q = 1 - \frac{1}{N\sigma^2} \sum_{i=1}^{L} N_i \sigma_i^2 \quad (5)$$

$$q_r = \left(1 - \frac{1}{N\sigma^2}\sum_{i=1}^{L} N_i\sigma_i^2\right)/S \quad (6)$$

In Equations (5) and (6), q is the explanatory power of factor X on the dependent variable Y. The range of values is [0, 1]. A larger value represents the stronger explanatory power of factor X. N represents the number of all samples, and N_i represents the number of samples within the partition; σ_i^2 is the variance of samples within the partition; i represents the partition, and L indicates the number of partitions; $i = 1, 2, \ldots, L$; q_r represents the relative contribution, and S indicates the area of the influencing factor.

- Interaction analysis of influence factors

The interactive detection module within GeoDetector was utilized to analyze the interactions among the influencing factors. In this study, this module was used to explore potential synergistic or antagonistic relationships between the independent and dependent variables (Table 2).

Table 2. Interaction detection types.

Interaction Types	Judgment Basis
Nonlinear weaken	$q(X_1 \cap X_2) < min[q(X_1), q(X_2)]$
Bivariable enhanced	$q(X_1 \cap X_2) > max[q(X_1), q(X_2)]$
Univariable weaken	$min[q(X_1), q(X_2)] < q(X_1 \cap X_2) < max[q(X_1), q(X_2)]$
Nonlinear enhanced	$q(X_1 \cap X_2) > q(X_1) + q(X_2)$
Independent	$q(X_1 \cap X_2) = q(X_1) + q(X_2)$

- Settings of influence factors and establishment of spatial relationships with dependent variables

The main aim of this study is to analyze the spatial pattern of EEQ and the underlying factors influencing its changes in the open-pit mining concentration area. Specifically, this study explores the impact of LUCC caused by urban expansion, mine development, and rehabilitation and treatment. Initially, eight land use/cover types, namely farmland, woodland, grassland, water area, unused land, construction land, mining land, and mining rehabilitation were used as influencing factor X. The RSEI value for a single year was used as the dependent variable Y for the identification of control factors governing the spatial pattern. Subsequently, the reciprocal transfer among land use/cover types were studied as the influencing factor X, with the change in EEQ over time serving as the dependent variable Y to explore the driving impact of LUCC on EEQ changes.

To establish the spatial correspondence between the impact factor and the dependent variable, we conducted a preprocessing step on both the impact factor and the dependent variable using type decomposition based on the abundance index and quantifying spatial dissimilarity [41]. The first step involved discretizing the study area using a grid-based approach. Subsequently, we calculated the areas covered by the impact factor X and the mean value of the dependent variable Y, all based on the grid cells. As the input for the GeoDetector model necessitates the impact factor X to be categorized, we divided the impact factor into five levels using the Jenks method.

- Analysis of the extent of spatial spillovers from changes in EEQ

LUCC will inevitably have an impact on the EEQ within the surrounding area [48]. We used ArcGIS 10.7 to explore the spatial spillover impact of LUCC on EEQ. This was done by assessing changes in ecological environment quality within buffer zones of different radii, ranging from 50 to 1000 m. These buffer zones were established based on the LUCC vector plane, both inside and outside polygon features. The buffer zones had radii set at

50 m intervals, and we utilized GIS to analyze the change in ecological quality within these buffer zones.

$$R_a = \frac{s_i}{s_b} \quad (7)$$

In Equation (7), S_i represents the area of EEQ change under the buffer area generated by a certain type of LUCC, S_b represents the buffer area, and R_a represents the proportion of the area of EEQ change in the buffer area. When the buffer zone reaches a certain extent, R_a will show a steady trend. This indicates that EEQ no longer has a spatial autocorrelation with LUCC, and the extent of the buffer zone at this point is its spatial spillover range.

3. Results

3.1. Temporal and Spatial Changes in Land Use/Cover

Figure 2 illustrates the results of the land use/cover classification conducted in this study. The northern and northwestern regions are characterized by flat terrains and are predominantly classified as suburban areas, mainly consisting of farmland. In contrast, the southern and eastern regions, which are remnants of Taishan Mountain, exhibit a more mountainous and higher terrain, and are predominantly covered by woodland and grassland. The mining land is mainly concentrated in the transition zone between the suburbs and the mountains, displaying a spatially distribution in a strip-like discrete manner.

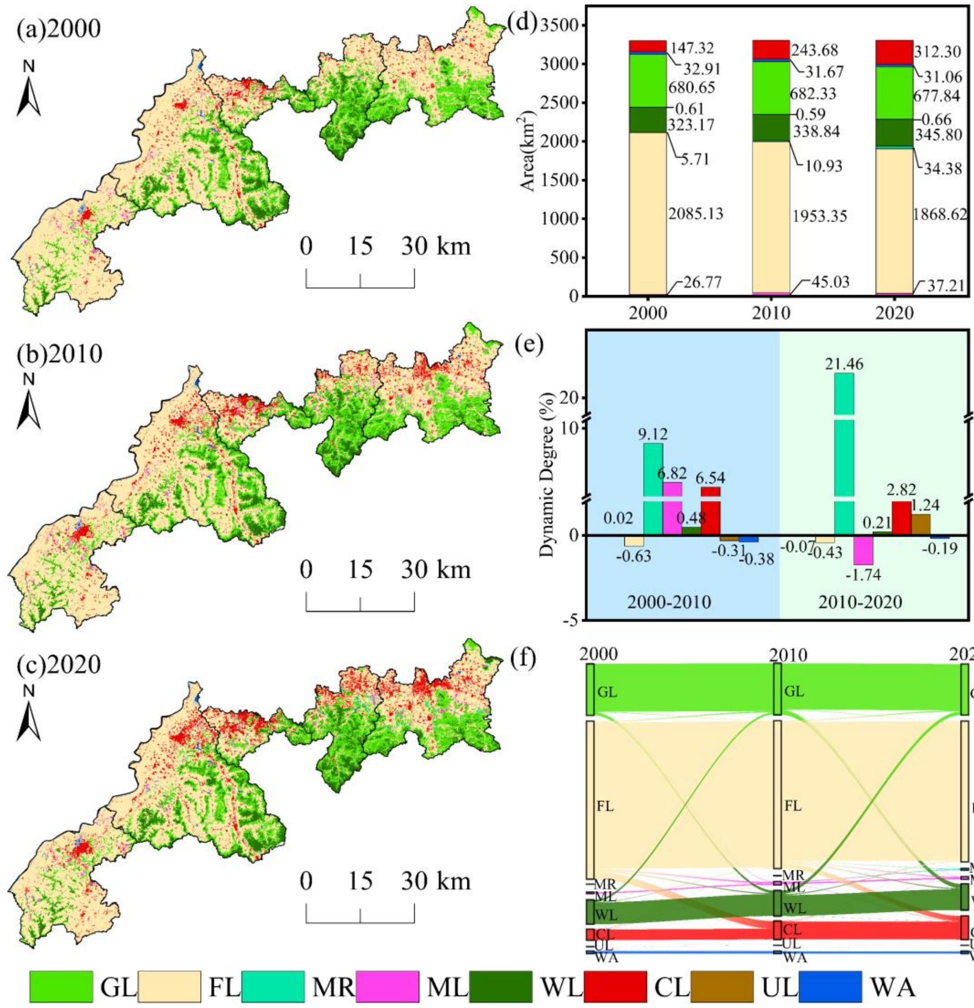

Figure 2. Land use/cover classification results. (**a**–**c**) Land use/cover status 2000–2020, (**d**) land use/cover area statistics results, (**e**) LUCC dynamic degree, and (**f**) LUCC Sankey diagram.

The overall land use/cover structure in the study area has exhibited relative stability over the past 20 years. Farmland continues to dominate as the prevailing land type, accounting for more than 1800 km^2 of the area. Woodland, grassland, water areas, and other land types with important ecological regulation functions, as well as mining land and mine rehabilitation areas, account for relatively smaller proportions.

The land use/cover types in the study area experienced intricate and uneven changes in their structure and spatial distribution during 2000–2020. According to the findings presented in Figure 3, the first 10 years, witnessed a notable increase of 96.36 km^2 in the construction land area, primarily attributed to urban expansion and human activities. However, the implementation of the ecological protection policy, specifically the "Returning Farmland to Forest and Grassland" initiative, resulted in the transformation of a substantial amount of farmland into woodland and grassland. Additionally, extensive ore mining during this period led to a significant expansion in the mining area. During the subsequent decade, the urban expansion of Jinan City persisted in encroaching on farmland and grassland, leading to further expansion of the construction land area. This phenomenon was predominantly observed in the transformation of a significant portion of farmland in the city's suburbs into construction land. It is noteworthy that in 2018, with the implementation of the mine geological environmental protection and treatment planning program in Shandong Province, a significant number of mining areas were closed, and abandoned mines underwent rehabilitation. Consequently, the mining land area decreased, while the corresponding area of mine rehabilitation experienced a significant increase. The implementation of environmental protection policies has played a pivotal role in driving the dynamic character of mine rehabilitation. Therefore, mine rehabilitation has become a highly dynamic type.

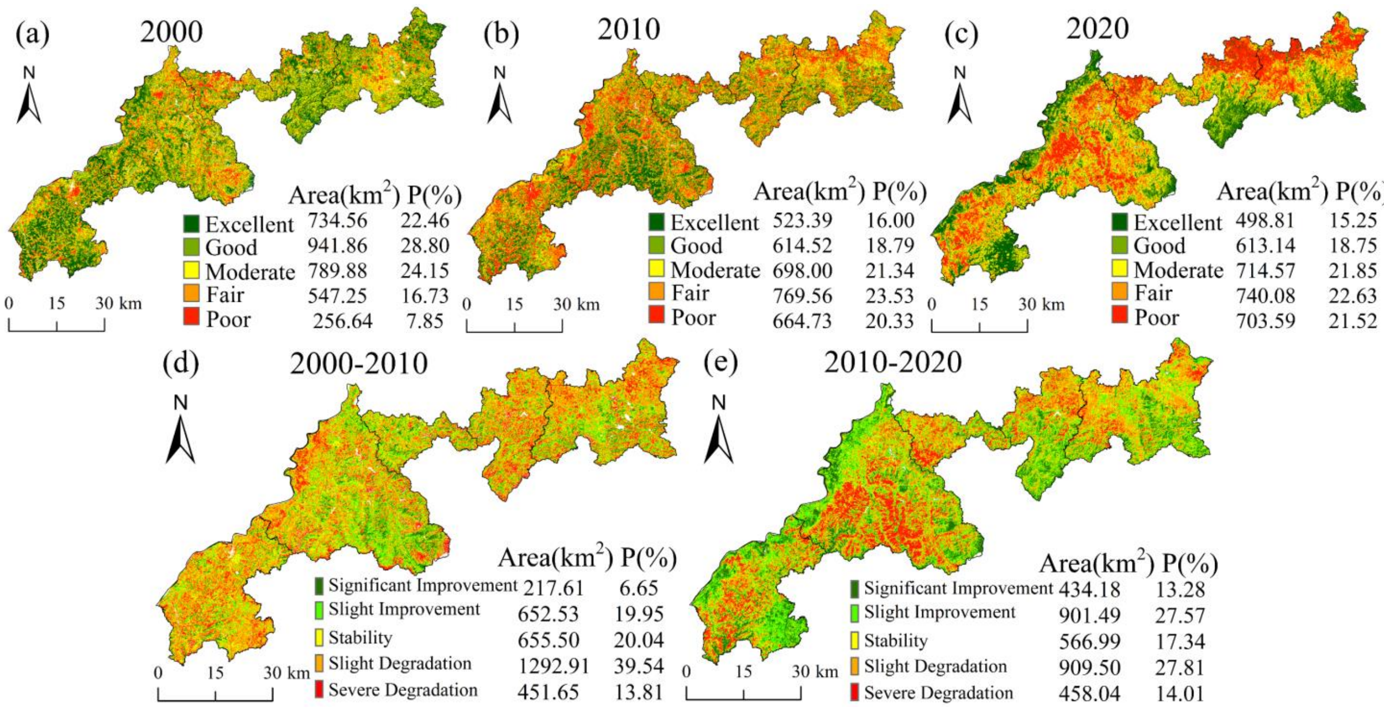

Figure 3. Spatial distribution and spatio-temporal changes in RSEI in the study area. (**a**–**c**) The spatial distribution of RSEI from 2000 to 2020, and (**d**,**e**) the spatial and temporal changes in RSEI from 2000 to 2020.

3.2. Response of EEQ to LUCC

Tables 3–5 reveal that PC1 and PC2 collectively contribute more than 90% to the RSEI from 2000 to 2020. Specifically, PC1's contribution rates in 2000, 2010, and 2020 are 82.02%, 83.4%, and 80.15%, all exceeding 80%. This suggests that PC1 primarily encompasses the characteristics of the four indicators. In contrast, PC2 to PC4 exhibit irregular eigenvalues and mixed positive and negative indicator loadings. However, PC1 stands out as NDVI and WET exhibit positive values, while NDBSI and LST indicate negative values, aligning with the known fact that greenness and moisture positively impact the ecosystem, while dryness and heat have adverse effects. Consequently, the use of PC1 for constructing the RSEI is justified. To facilitate the assessment, the normalized PC1 values were classified into five grades according to the existing grading criteria [49,50] at 0.2 numerical intervals. The values were taken in the range of [0, 0.2), [0.2, 0.4), [0.4, 0.6), [0.6, 0.8), [0.8, 1.0], corresponding to ecological quality levels in the order of poor, fair, moderate, good, and excellent. The area and proportion of each ecological class for each year were also calculated.

Table 3. Principal component analysis of RSEI in 2000.

Index	PC1	PC2	PC3	PC4
NDVI	0.749	−0.185	0.362	0.523
WET	0.362	0.326	−0.852	0.180
NDBSI	−0.543	0.056	−0.034	0.832
LST	−0.060	−0.924	−0.371	0.013
Eigenvalue	0.256	0.027	0.025	0.003
Contribution rate /%	82.02	9.12	8.18	0.68
Cumulative contribution rate /%	82.02	91.14	99.32	100

Table 4. Principal component analysis of RSEI in 2010.

Index	PC1	PC2	PC3	PC4
NDVI	0.697	0.168	−0.435	−0.537
WET	0.006	−0.143	−0.786	0.602
NDBSI	−0.715	0.214	−0.434	−0.508
LST	−0.032	−0.950	−0.053	−0.304
Eigenvalue	0.266	0.043	0.009	0.003
Contribution rate /%	84.42	11.85	3.03	0.70
Cumulative contribution rate /%	84.42	96.27	99.30	100

Table 5. Principal component analysis of RSEI in 2020.

Index	PC1	PC2	PC3	PC4
NDVI	0.755	−0.180	0.336	0.528
WET	0.302	0.915	−0.251	0.037
NDBSI	−0.553	0.308	0.537	0.554
LST	−0.161	−0.173	−0.732	0.646
Eigenvalue	0.248	0.049	0.011	0.002
Contribution rate /%	80.15	15.54	3.23	1.08
Cumulative contribution rate /%	80.15	95.69	98.92	100

Based on the statistical results of the RSEI of the study area (Figure 3), it can be concluded that the total sum of the area occupied by excellent, good and moderate EEQ in the study area reached 75.41% in 2000. This indicates a favorable overall EEQ for that period. However, by 2010, the area of poor and fair amounted to 769.56 km^2 and 664.73 km^2, indicating that the ecological quality of the study area had been degraded during these 10 years, dominated by slight deterioration and comprising 39.54% of the total area. Continuing to 2020, the area proportions of each level of EEQ showed no significant changes in comparison to 2010. Nevertheless, the areas of the study area with slightly better and significantly better EEQ in these 10 years have increased compared with the previous 10 years, with an increase of 248.96 km^2 and 216.57 km^2, respectively. This indicates a significant improvement in the ecological environment quality within the study area. However, the spatial differentiation of the ecological environment quality change pattern in the study area is more obvious. By 2020, the EEQ in the study area appears to be developing in a polarized manner.

3.3. Impact of Land Use/Cover Distribution on the Spatial Pattern of EEQ

When conducting GeoDetector analysis, it is essential to consider the scale effect of the data. In this study, we conducted scale effect experiments at 500 m intervals, ranging from 500 m to 5000 m. The results (see Figure 4) demonstrate that the q value of the factors exhibit relatively stable patterns within the range of [3,4] km, while they demonstrate greater volatility outside this interval. Furthermore, the p value results indicate that the p value of some factors began to increase after 3 km, leading to insignificant results, whereas all factors had significant p value at 3 km. Therefore, a 3 km scale was chosen as the optimal scale for analysis.

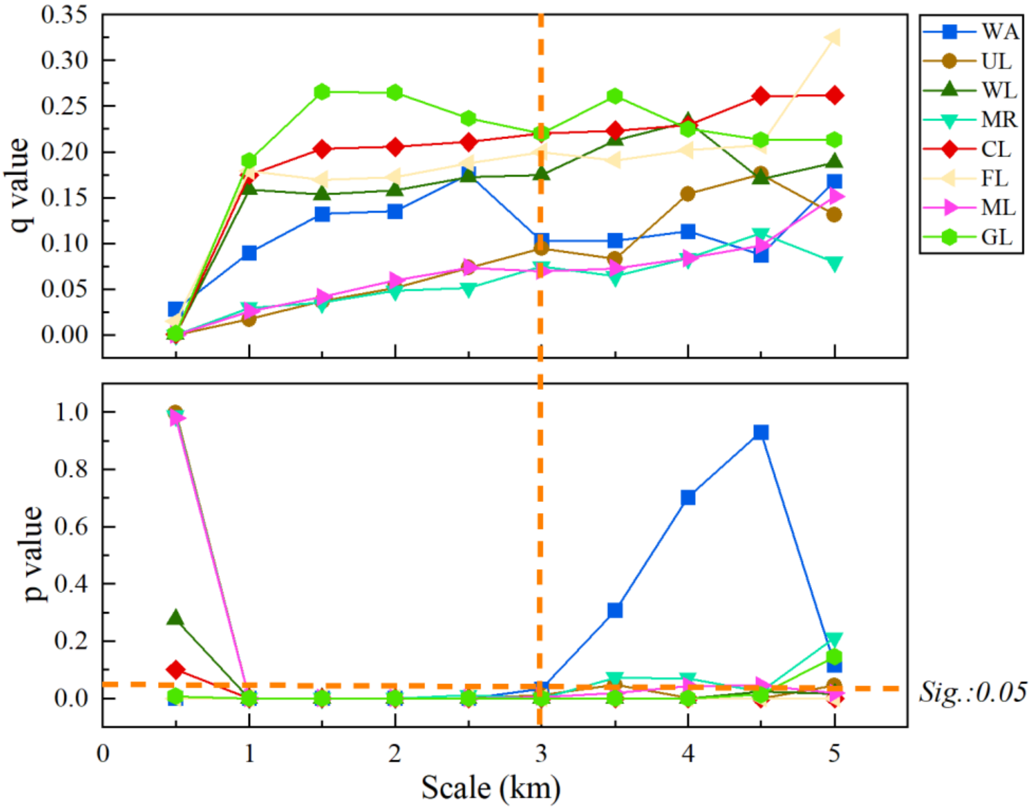

Figure 4. Results of scale effect analysis.

Figure 5a illustrates the results of factor detection. Construction land, grassland, and farmland demonstrate stronger explanatory power, highlighting that the spatial distribution of EEQ in the study area is predominantly influenced by these land categories. In contrast, the impact of mining land is less pronounced, mainly because of its relatively limited extent.

Figure 5b–d illustrates the detection results of factor interactions. Construction land ∩ woodland exhibits the strongest explanatory power on the spatial pattern of EEQ in the study area, although the interaction types holding the top five positions in explanatory power have exhibited fluctuating changes over the last 20 years, with interactions among woodland, grassland, water, and mining land exerting a considerably stronger influence on the spatial pattern of EEQ. Particularly in 2020, the influence of the interactions between different land use type on the EEQ has been enhanced.

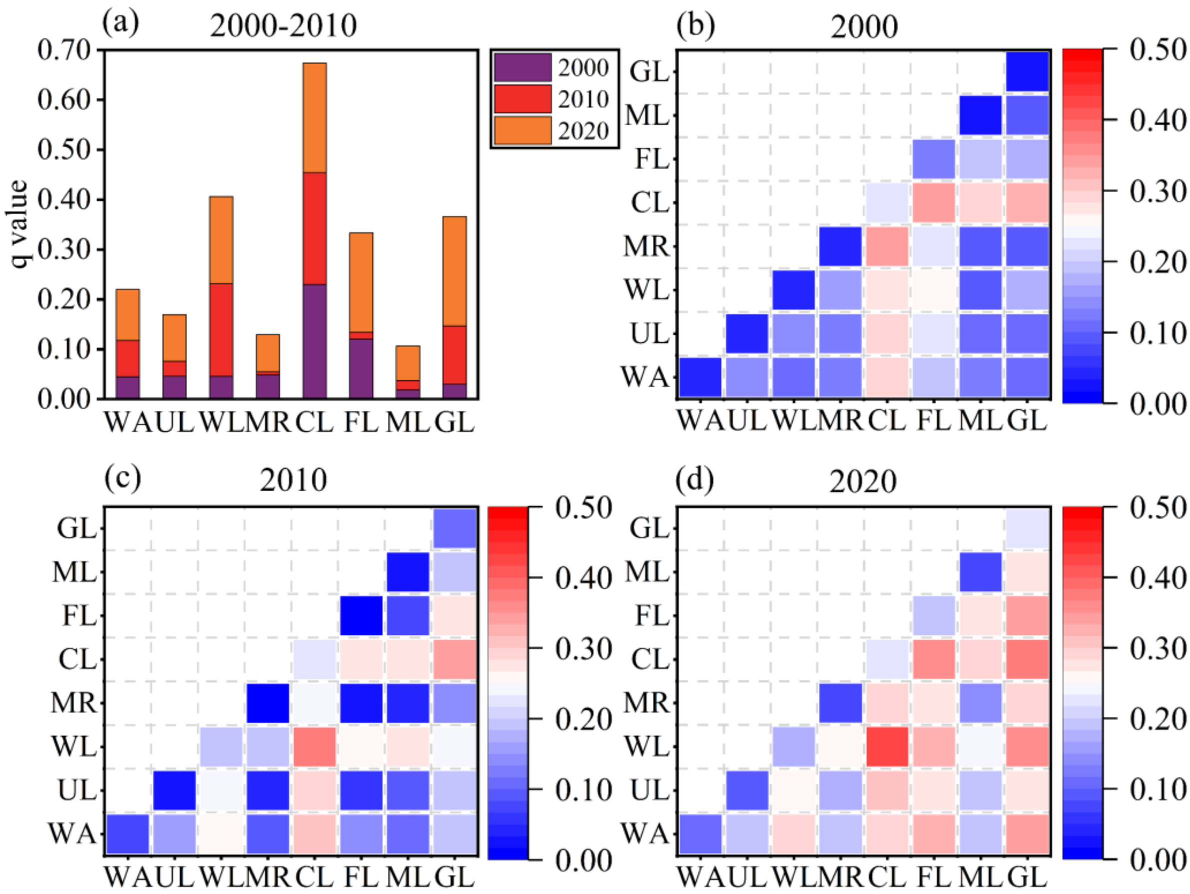

Figure 5. Results of the detection of RSEI spatial pattern influence factors. (**a**) The factor detection result for 2000, 2010 and 2020, (**b**) the factor interaction detection result in 2000, (**c**) the factor interaction detection result in 2010, and (**d**) the factor interaction detection result in 2020. The stronger the interaction between the two influencing factors, the redder the hue in the figure, while a weaker interaction is indicated by a bluer hue.

3.4. Driving Effect of LUCC on EEQ Change

We conducted factor detection and interaction detection using 3 km-scale grids to explore the influence mechanisms of LUCC on EEQ improvement and deterioration for the periods of 2000–2010 and 2010–2020, respectively.

3.4.1. Absolute Influencing Factors of EEQ Change

Figures 6 and 7 reveal that farmland → construction land, farmland → grassland, grassland → farmland, and mining land → mining rehabilitation significantly contribute to the EEQ change from 2000 to 2020. In addition, Figure 8 demonstrates that the interactions farmland → grassland ∩ mining land → mining rehabilitation, farmland → grassland ∩ farmland → woodland, and farmland → woodland ∩ mining land → mining rehabilitation play a crucial role in improving the EEQ during this period. This indicates that the transformation of farmland to woodland and grassland, as well as the transformation of mining land to mine rehabilitation, have had a positive influence on the greenness and a reduction in heat in the area, thereby contributing to the improvement of the EEQ. Conversely, the interactions farmland → construction land ∩ grassland → farmland, grassland → construction land ∩ grassland → farmland, and farmland → mining land ∩ grassland → mining land, which exhibit stronger explanatory power for EEQ degradation, indicate that the transformation of farmland to construction land, the transformation of grassland to farmland, and mining activities have led to increased regional dryness and heat. These interactions have exacerbated the degradation of EEQ during this period.

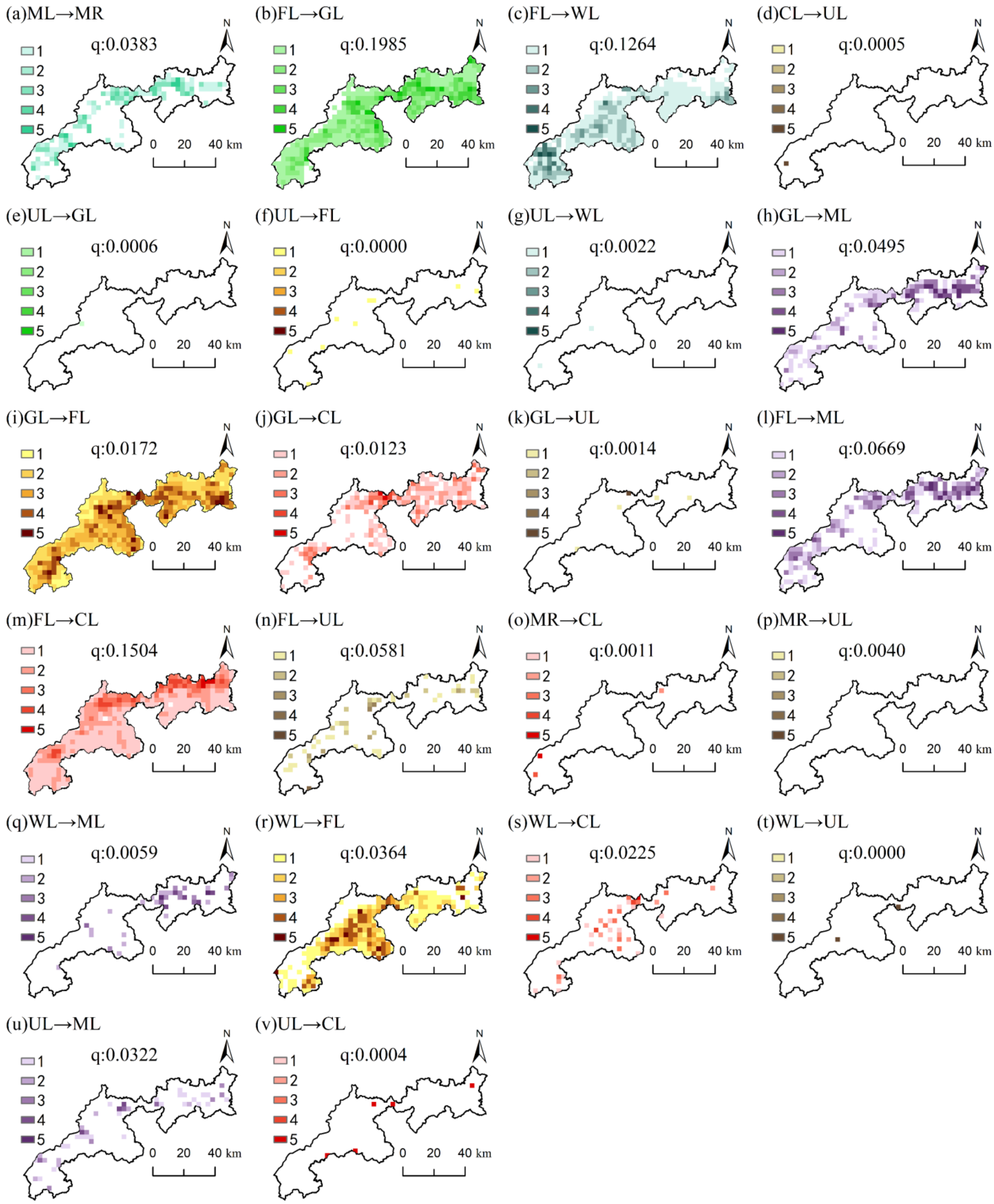

Figure 6. Impact factors detection of RSEI changes from 2000 to 2010.

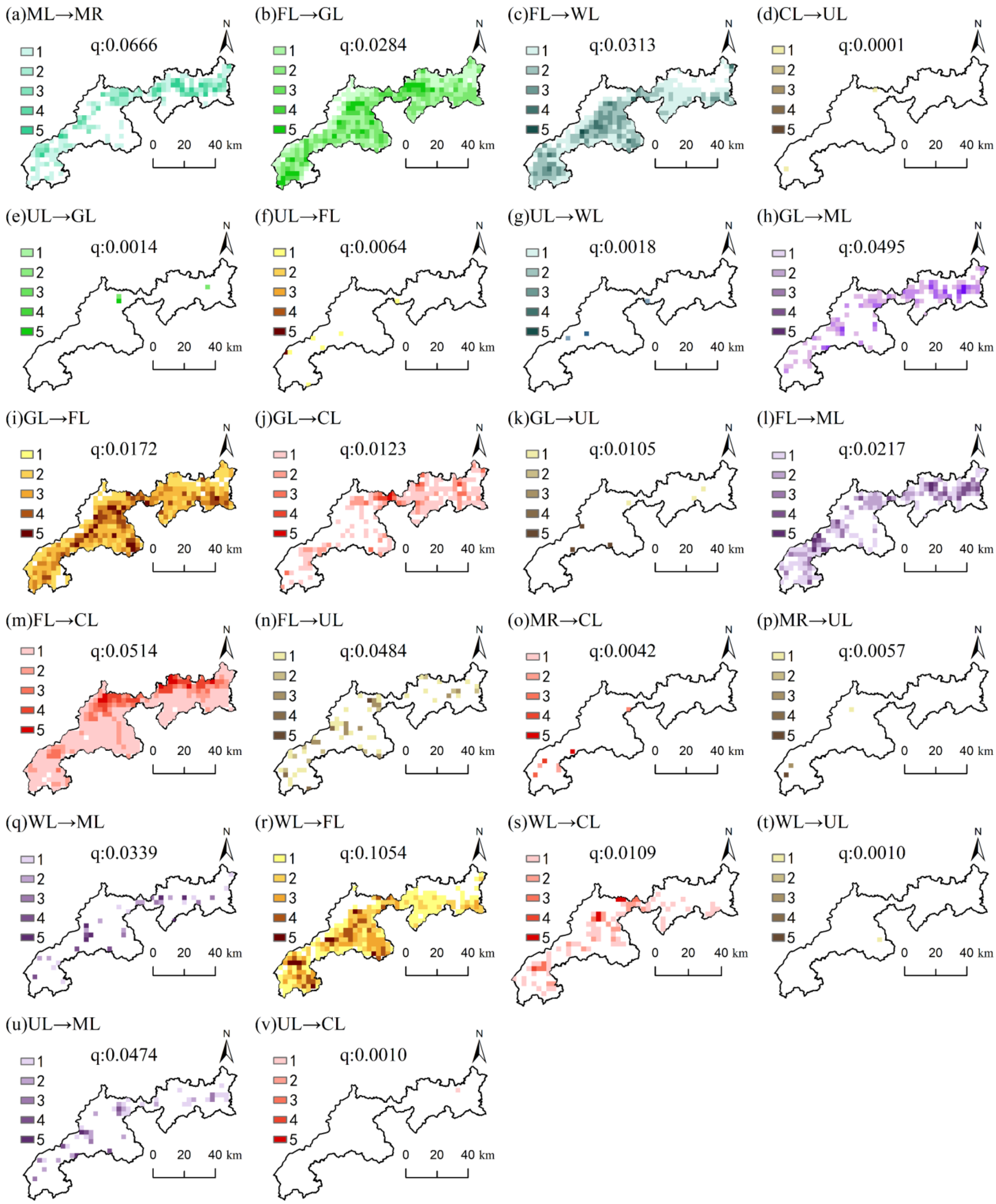

Figure 7. Impact factors detection of RSEI changes from 2010 to 2020.

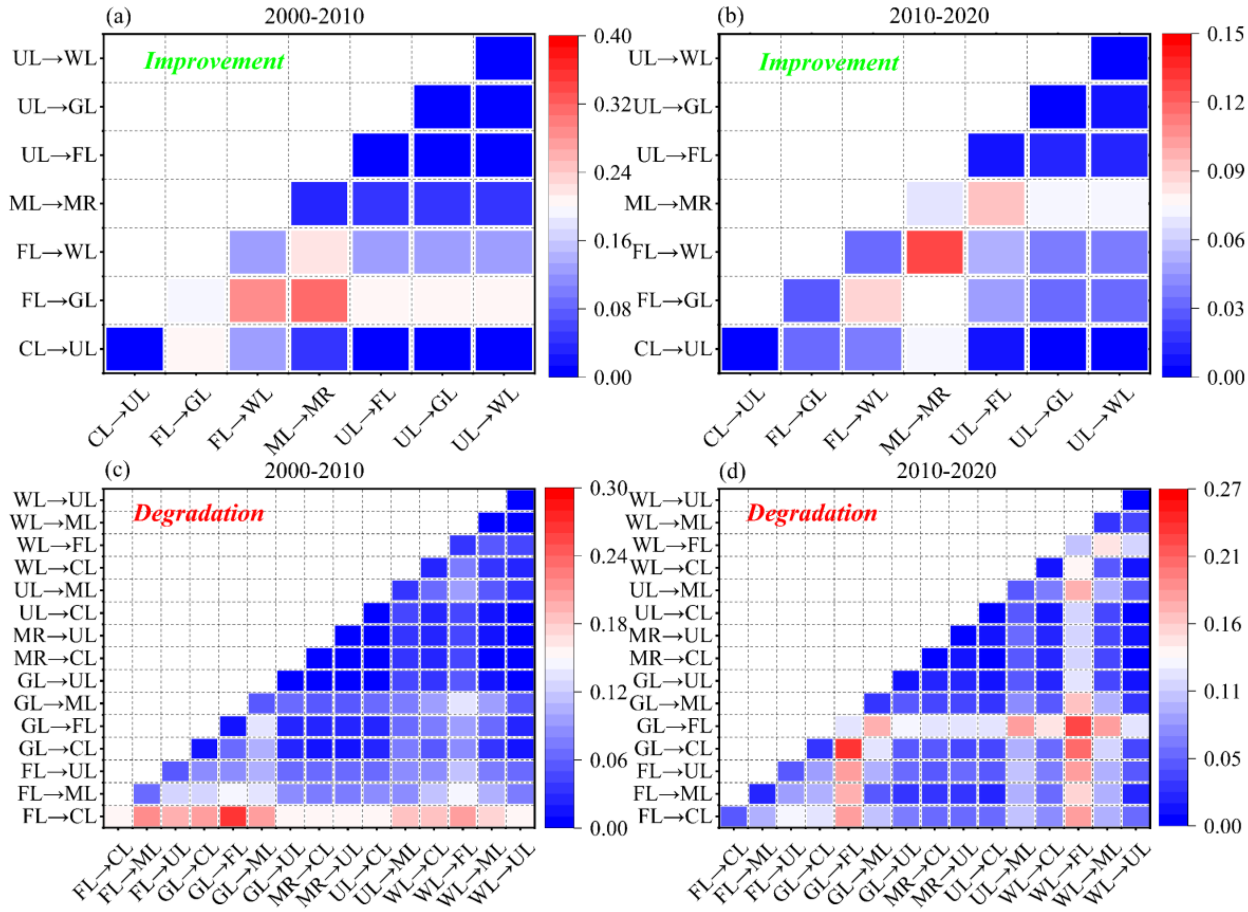

Figure 8. The interaction of driving factors of RSEI changes. (**a**) The interaction of the driving factors for improving the EEQ from 2000 to 2010, (**b**) the interaction of the driving factors for improving the EEQ from 2010 to 2020, (**c**) the interaction of the driving factors for degrading the EEQ from 2000 to 2010, and (**d**) the interaction of the driving factors for degrading the EEQ from 2010 to 2020. The stronger the interaction between the two influencing elements, the redder the hue in the figure, and the opposite is shown for weaker interactions.

3.4.2. Relative Influencing Factors of EEQ Change

We further measured the relative contribution of factors with a significant absolute impact. The results show that from 2000 to 2020 (Figure 9), the mining land → mining rehabilitation has better explanatory power in improving the EEQ, with q_r value of 0.0735 and 0.0291, respectively. This indicates that the remediation of mining land plays an important role in improving the EEQ. Furthermore, the grassland → mining land and farmland → mining land are predominantly land use/cover types contribute to the deterioration of EEQ, with q_r value of 0.0090, 0.0032, and 0.0184, respectively. This indicates that some ore mining activities have a relatively stronger influence on the deterioration of EEQ.

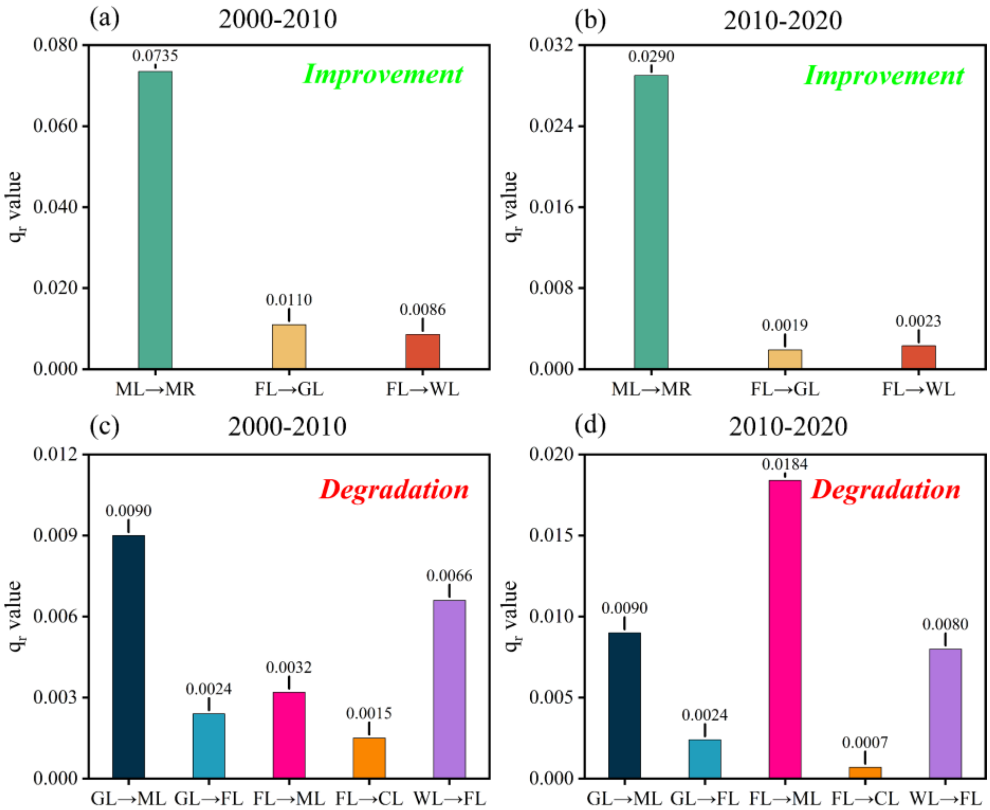

Figure 9. The results of relative contribution. (**a**) The relative contribution of the drivers of EEQ improvement from 2000 to 2010, (**b**) the relative contribution of the drivers of EEQ improvement from 2010 to 2020, (**c**) the relative contribution of the drivers of EEQ degradation from 2000 to 2010, and (**d**) the relative contribution of the drivers of EEQ degradation from 2010 to 2020.

3.4.3. Analysis of Spatial Spillover Effects of Changes in EEQ

On the basis of the previous analysis, we analyzed the spatial spillover effect of factors with important influence roles. We established buffer zones with radii ranging from 50 m to 1000 m and conducted spatial spillover effect experiments at 50 m intervals. As can be seen in Figure 10, the proportion of both improvement and deterioration of EEQ gradually decreases and stabilizes as the buffer zone range increases. Nevertheless, variations exist in the spatial spillover range of the influences of different factors on EEQ changes. Regarding the factors contributing to EEQ enhancement, the spatial spillover ranges of farmland → woodland, mining land → mining rehabilitation and farmland → grassland are 300 m–550 m, 500 m–550 m, and 700 m, respectively. This indicates that the implementation of ecological protection policies has promoted the expansion of ecological land use areas, enhanced their service functions, and consequently improved the EEQ within the surrounding region. Regarding the factors contributing to EEQ deterioration, the spatial spillover range of grassland → mining land is 100 m, farmland → mining land spans 250 m–400 m, woodland → farmland extends to 400 m, grassland → farmland reaches 800 m, and farmland → construction land encompasses 950 m–1000 m. It can be seen by comparison that the impacts of ecological land destruction may have a greater extent of impact on the deterioration of the surrounding ecological environment quality.

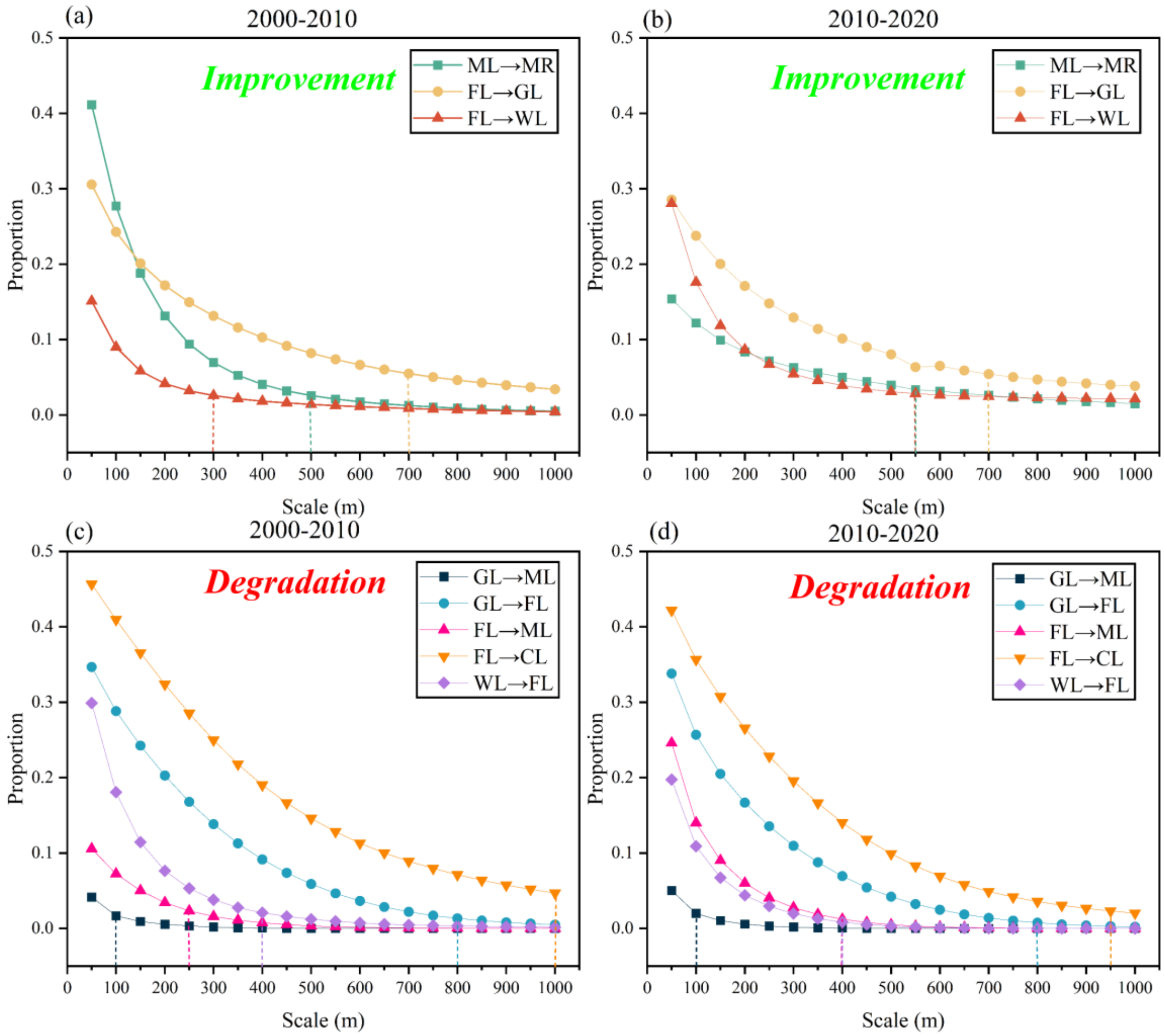

Figure 10. Spatial spillover results of LUCC on RSEI changes under different buffer radii from 2000 to 2020. (**a**) The spatial spillover effect of EEQ improvement in 2000–2010, (**b**) the spatial spillover effect of EEQ improvement in 2010–2020, (**c**) the spatial spillover effect of EEQ degradation in 2000–2010, and (**d**) the spatial spillover effect of EEQ degradation in 2010–2020.

4. Discussion

4.1. Coupled Effects of Urban Expansion and Mining Activities on LUCC

The land use/cover structure within the study area has exhibited a relatively stable pattern over the past two decades. Farmland and construction land remain the dominant land use/cover types, while land types with ecological importance, such as woodland, grassland, mining land, and mine rehabilitation land, are relatively limited. These findings align with the research conducted by Wang et al. [41]. However, a more complex situation emerges regarding the changing dynamics among different land types, as illustrated in Figure 3. This changing pattern is mainly influenced by urban expansion activities in different urban development stages [51], the land demand driven by mining activities [52], and relevant ecological protection policies [41].

Specifically, between 2000 and 2010, Jinan City formulated a master land use plan (2001–2020) that set the development direction for Jinan City and promoted the progress of the urbanization construction phase. As a result, numerous townships underwent expansion, leading to a significant reduction in farmland and rapid expansion of construction land. Simultaneously, the area was abundant in mineral resources, which supplied a significant quantity of resources for Jinan's urbanization, leading to a considerable expansion of mining land. However, the encroachment of urbanization development on other land uses [53] surpassed the scale of mining development, thereby becoming the primary driver of land use/cover changes. Subsequently, between 2010 and 2020, Jinan City implemented successive urban planning policies to promote urban renewal and industrial transfer [54], aiming to enhance spatial use efficiency. This further led to the occupancy of a significant portion of farmland, resulting in a rapid trend of farmland reduction [55].

Over the past two decades of urbanization, the expansion of urban land has encroached upon ecological and productive land that the large and rapid growth of urbanized land occurred at the expense of a substantial proportion of farmland and green space [56]. However, during this period, Jinan also implemented several ecological protection policies, such as the "Return of Farmland to Forest and Grassland" and the "Mine Environment Management and Protection Plan". These policies led to the transformation of a sizable portion of farmland and mining land to grassland and woodland. In addition, Jinan City follows the "simultaneous mining and rehabilitation" principle, which safeguards production requirements while simultaneously advancing environmental protection and treatment. The implementation of these policies has, to some extent, alleviated the adverse impacts of urbanization and mining development on EEQ and land use/cover. This serves as a positive exploration and example of sustainable development.

4.2. Impact of LUCC on Changes in EEQ

After over 20 years of LUCC, the overall EEQ has exhibited a sustained decrease, with the proportion of places with poor EEQ reached 21.52%. Notably, the spatial distribution of EEQ gradually transitioned from fragmentation to agglomeration, particularly evident in 2020, indicating obvious spatial heterogeneity and agglomeration effects in the distribution of good and poor EEQ (Figure 3). These phenomena can be attributed to multiple factors.

Firstly, the spatial expansion of urbanization development has exacerbated the heat island effect [57], while mining development has inflicted serious damage to regional land surfaces [44], both contributing to the gradual deterioration of EEQ. Unsustainable land use and over-exploitation during the urbanization process have exerted pressure on the ecosystem and significant spatial spillover effects in the surrounding area, serving as the underlying causes of ecological damage and quality deterioration. Secondly, the implementation of environmental protection policies in the southern mountainous areas [58] and mining concentrations has contributed to the improvement of EEQ in the local area, and activities such as mine rehabilitation have exerted further influence on the EEQ of their surrounding areas. These policies have partially mitigated the declining trend of EEQ in the study area by limiting mining activities and strengthening ecological protection measures. However, this has not completely mitigated the agglomeration effect of EEQ degradation, primarily due to the spatial unevenness of urbanization development, mining development, and ecological protection implementation.

Furthermore, our findings indicate that changes in predominant land types, such as farmland and construction land, which cover larger areas, have a significant influence on the changes in EEQ. However, changes in non-dominant land types, such as mining activities and mine rehabilitation, played a relatively more significant role in influencing the EEQ [59]. Among them, mining land → mining rehabilitation has a lower q value compared to farmland → grassland and farmland → woodland, but its q_r value is significantly higher than that of farmland → grassland and farmland → woodland. Similarly, grassland → mining land and farmland → mining land have a lower q value compared to farmland → construction land and woodland → farmland, but their q_r value are significantly higher than those of farmland → construction land and woodland → farmland. This indicates that mining activities have caused damage to the ecological environment, while also validating the effectiveness of ecological environmental protection policies and measures, such as mine rehabilitation, in improving the ecological environment. However, we observe that the spatial spillover effects of these ecological improvements on EEQ do not completely offset the spatial spillover effects of ecological damage. Therefore, it is crucial to strengthen the control of mining activities in suburban open-pit mining concentrations and improve the methods and quality of mine rehabilitation. These tasks are essential and significant components of ecological environmental protection and rehabilitation efforts.

4.3. Countermeasures for the Development and Ecological Protection of Suburban Land and Mineral Resources

To cope with the coupled impact of urbanization and mining development on the ecological environment, targeted management measures need to be proposed. Firstly, it is essential to implement a rational urban land planning strategy that promotes economical and intensive approaches, with a meticulous demarcation of urban land expansion limits. Proactive changes are necessary to modify the ecological spatial arrangement in order to narrow the divide between urban and rural ecological development. This approach can help reduce the occupation of land with valuable ecological services by urban construction, thereby mitigating the spatial aggregation effect of EEQ degradation. Secondly, there is a need to strengthen mine rehabilitation efforts, including the ecological restoration of historical and production mines. Diversified mine rehabilitation methods should be adopted, ecological restoration strategies tailored to local conditions should be implemented. Additionally, a long-term evaluation mechanism for ecological restoration and management should be established to enhance the quality and effectiveness of mine ecological restoration and management. Thirdly, as one of the central cities in the Yellow River Basin focusing on ecological protection and high-quality development, Jinan should strictly adhere to the ecological red line and safeguard the bottom lines. This involves establishing protected areas for the conservation of natural resource in suburban regions and designating prohibited development zones, which must be integrated into regional territorial spatial planning. These measures aim to prevent the infringement of natural resources and the ecological environment in suburban areas resulting from urban expansion and mineral development. At the same time, it is crucial to strengthen a robust ecological compensation system to prevent ecological beneficiaries from avoiding their ecological responsibilities. This system will help maintain and guarantee the rehabilitation and sustainable development of the suburban ecological environment in Jinan.

4.4. Limitations and Prospects

In comparison to previous studies on the impact of LUCC on RSEI [41], this study provides an advantage by introducing a relative contribution index to quantify the contribution of non-dominant land types. By utilizing the q_r value, the issue of area-influenced factor detection in GeoDetector was addressed. The introduction of this index reveals the important influence of changes in non-dominant land use/cover types, such as mining land and mine rehabilitation, on changes in EEQ. The index serves as a supplement to assess how suburban LUCC affects EEQ. Building upon this foundation, our study used the buffer zone analysis method to measure the spatial spillover effects of several important LUCC affecting EEQ, which will provide a reference for the study of the spatial spillover effects of LUCC.

However, the LUC classification system used in this study still has certain shortcomings, particularly in the vicinity of mining areas. Ore processing facilities and stockpiles may yield different impacts on EEQ compared to individual mining pits. Therefore, future studies should analyze the impacts of LUCC on EEQ in suburban open-pit mining concentrations using a more detailed and accurate classification system. Additionally, the study area involves the Yellow River, the Daqing River, as well as numerous lakes and reservoirs. Water areas often exhibit distinct reflectance and absorption characteristics in remote sensing data, which can lead to anomalous values of RSEI [60]. Therefore, for an accurate assessment terrestrial EEQ, future study should explore the EEQ assessment method specifically designed for water areas. Furthermore, although ecological rehabilitation treatments have partially alleviated ecosystem fragmentation, some fragmented ecological nodes persist. These ecological nodes play are crucial role in connecting and preserving regional ecosystem functions [61]. Consequently, it is crucial to further explore the relationship between changes in ecological nodes and EEQ to provide guidance for ecological protection and coordinated development in suburban areas.

5. Conclusions

Urbanization and mining activities are the main drivers of LUCC in suburban open-pit mining development areas, leading to changes in EEQ. Understanding the coupled mechanisms of these changes is crucial for promoting sustainable development in these areas and formulating effective ecological protection policies. In this study, a typical open-pit mining concentration area on the outskirts of Jinan City was selected as the study area, and the impact of coupled urbanization and mining development on LUCC on EEQ was investigated. To measure the impact of non-dominant land use/cover type changes, a relative contribution value index was designed, and the spatial impacts of LUCC on changes in EEQ were explained in conjunction with buffer zone analysis. The results show that the spatial distribution of EEQ is mainly influenced by the dominant land types, including construction land, grassland, and farmland. However, the changes in non-dominant land use/cover types, including mining land and mine rehabilitation, play a relatively stronger role in driving EEQ changes. The transformation of farmland to construction land and grassland and woodland to farmland during the past 20 years has been the main factors leading to ecological degradation in the study area. Meanwhile, the relative impact of the conversion of woodland to mining land, caused by mining, on ecological degradation cannot be ignored. Conversely, the transformation of farmland to woodland and grassland stands as the primary driver of EEQ improvement. Notably, mining rehabilitation has played a significant role in improving the EEQ of the local area. However, the uneven distribution of LUCC continues to negatively affect overall EEQ and exacerbates the spatial aggregation effects. Additionally, the spatial spillover effects of ecological improvement measures have not been able to compensate for the spatial spillover effects of ecological damage.

Therefore, we suggest controlling urban expansion and optimizing mine rehabilitation measures to adjust the ecological spatial structure, along with establishing robust ecological compensation mechanisms to effectively preserve and protect the ecological environment in suburban open-pit mining concentration areas.

However, further research is essential to enhance the land use/cover classification system, develop EEQ assessment methods for water areas, and explore the mechanisms linking changes in ecological nodes to EEQ. These efforts will advance ecological protection and promote the coordinated development of suburban areas.

Author Contributions: Conceptualization, H.L. and Q.W.; methodology, H.L. and N.L.; software, N.L.; validation, H.Z., Y.T. and Z.Z.; formal analysis, H.L. and Q.W.; investigation, H.Z. and Y.T; resources, H.Z., Y.T. and Z.Z.; data curation, H.Z., Y.T. and Z.Z.; writing—original draft preparation, H.L. and Q.W.; writing—review and editing, Q.W. and N.L.; visualization, H.Z.; supervision, N.L.; project administration, Q.W. and N.L.; funding acquisition, Q.W. and N.L. All authors have read and agreed to the published version of the manuscript.

Funding: This work was funded by the Ph.D. Programs Foundation of Shandong Jianzhu University (XNBS1984) and the Fundamental Research Program of Shandong Collaborative Innovation Center for Smart City (003160401).

Data Availability Statement: Not applicable.

Acknowledgments: The authors are grateful to the USGS for providing the Landsat images, the Urban Ecology Big Data Analysis and Modeling Research Group for providing data and technical support, and the State Key Laboratory of Resources and Environmental Information System (SKLREIS), Institute of Geographic Sciences and Natural Resources Research, Chinese Academy of Sciences (IGSNRR, CAS) for providing the software technical support.

Conflicts of Interest: The authors declare no conflict of interest.

Appendix A

- The wetness index

RSEI employs the wetness components obtained through the Kauth–Thomas transformation to assess the wetness of soil and vegetation. For ETM+ sensors and OLI sensors, there are differences in the calculated parameters of image wetness. Their equations are as follows:

$$WET_E = 0.2626\rho_{e1} + 0.2141\rho_{e2} + 0.0926\rho_{e3} + 0.0656\rho_{e4} - 0.7629\rho_{e5} - 0.5388\rho_{e7} \quad (A1)$$

$$WET_O = 0.1511\rho_{o2} + 0.1972\rho_{o3} + 0.3283\rho_{o4} + 0.3407\rho_{o5} - 0.7117\rho_{o6} - 0.4559\rho_{o7} \quad (A2)$$

In Equations (A1) and (A2), ρ_{e1} and ρ_{o2} represents the blue band, ρ_{e2} and ρ_{o3} represents the green band, ρ_{e3} and ρ_{o4} represents the red band, ρ_{e4} and ρ_{o5} represents the NIR band, ρ_{e5} and ρ_{o6} represents the SWIR band 1, and ρ_{e7} and ρ_{o7} represents the SWIR band 2.

- The greenness index

RSEI uses the Normalized Difference Vegetation Index (NDVI) as a metric to characterize the vegetation coverage within the study area. The calculation formula for NDVI is as follows:

$$NDVI = \frac{\rho_{nir} - \rho_{red}}{\rho_{nir} + \rho_{red}} \quad (A3)$$

In Equation (A3), ρ_{nir} represents the NIR band and ρ_{red} represents the red band.

- The heat index

The heat index in RSEI is defined by the surface temperature. To calculate the surface temperature, the Landsat User's Manual model is employed, taking into account the necessary correction parameters. The formula to express the surface temperature is as follows:

$$Lst = \frac{T_b}{\left[\frac{1+\varepsilon\lambda T_b}{\rho}\right]} - 273.15 \quad (A4)$$

$$T_b = \frac{K_2}{\ln\left(\frac{K_1}{L_t} + 1\right)} \quad (A5)$$

$$L_t = gain \times DN + bias \quad (A6)$$

In Equations (A4)–(A6), λ represents the thermal infrared band's central wavelength; $\rho = 1.438 \times 10^{-2}$ m; ε represents the emissivity, which is obtained by NDVI thresholding [62]; K_1 and K_2 are calibration parameters after radiation calibration; T_b represents brightness temperature; DN is the pixel's gray value; $gain$ and $bias$ are obtained from the image header file; L_t represents the Landsat thermal infrared wavelength band radiation value. Lst represents the surface temperature.

- The dryness index

The dryness index is composed of the building index (IBI) and the bare soil index (SI), abbreviated as NDBSI (Equation (A7)–(A9)). Its equation is:

$$NDBSI = \frac{SI + IBI}{2} \quad (A7)$$

$$SI = \frac{[(\rho_{swir1} + \rho_{red}) - (\rho_{nir} + \rho_{blue})]}{[(\rho_{swir1} + \rho_{red}) + (\rho_{nir} + \rho_{blue})]} \quad (A8)$$

$$IBI = \frac{\frac{2\rho_{swir1}}{\rho_{swir1}+\rho_{nir}} - \left[\frac{\rho_{nir}}{\rho_{nir}+\rho_{red}} + \frac{\rho_{green}}{\rho_{swir1}+\rho_{green}}\right]}{\frac{2\rho_{swir1}}{\rho_{swir1}+\rho_{nir}} + \left[\frac{\rho_{nir}}{\rho_{nir}+\rho_{red}} + \frac{\rho_{green}}{\rho_{swir1}+\rho_{green}}\right]} \quad (A9)$$

In Equations (A7)–(A9), ρ_{blue} represents the blue band, ρ_{green} represents the green band, ρ_{red} represents the red band, ρ_{nir} represents the NIR band, and ρ_{swir1} represents the SWIR band1.

References

1. Wu, J.; Xiang, W.-N.; Zhao, J. Urban ecology in China: Historical developments and future directions. *Landsc. Urban Plan.* **2014**, *125*, 222–233. [CrossRef]
2. Zhou, X.; Chen, H. Impact of urbanization-related land use land cover changes and urban morphology changes on the urban heat island phenomenon. *Sci. Total Environ.* **2018**, *635*, 1467–1476. [CrossRef] [PubMed]
3. Wang, J.; Da, L.; Song, K.; Li, B.-L. Temporal variations of surface water quality in urban, suburban and rural areas during rapid urbanization in Shanghai, China. *Environ. Pollut.* **2008**, *152*, 387–393. [CrossRef] [PubMed]
4. Shi, P.-J.; Yuan, Y.; Zheng, J.; Wang, J.-A.; Ge, Y.; Qiu, G.-Y. The effect of land use/cover change on surface runoff in Shenzhen region, China. *Catena* **2007**, *69*, 31–35. [CrossRef]
5. Xu, Y.; Luo, D.; Peng, J. Land use change and soil erosion in the Maotiao River watershed of Guizhou Province. *J. Geogr. Sci.* **2011**, *21*, 1138–1152. [CrossRef]
6. Concepción, E.D.; Moretti, M.; Altermatt, F.; Nobis, M.P.; Obrist, M.K. Impacts of urbanisation on biodiversity: The role of species mobility, degree of specialisation and spatial scale. *Oikos* **2015**, *124*, 1571–1582. [CrossRef]
7. Chen, X.; Liu, C.; Yu, X. Urbanization, Economic Development, and Ecological Environment: Evidence from Provincial Panel Data in China. *Sustainability* **2022**, *14*, 1124. [CrossRef]
8. Barral, M.P.; Benayas, J.M.R.; Meli, P.; Maceira, N.O. Quantifying the impacts of ecological restoration on biodiversity and ecosystem services in agroecosystems: A global meta-analysis. *Agric. Ecosyst. Environ.* **2015**, *202*, 223–231. [CrossRef]
9. Ning, L.; Jiayao, W.; Fen, Q. The improvement of ecological environment index model RSEI. *Arab. J. Geosci.* **2020**, *13*, 403. [CrossRef]
10. Zhu, D.; Chen, T.; Wang, Z.; Niu, R. Detecting ecological spatial-temporal changes by Remote Sensing Ecological Index with local adaptability. *J. Environ. Manag.* **2021**, *299*, 113655. [CrossRef]
11. Wang, S.; Zhuang, Y.; Cao, Y.; Yang, K. Ecosystem Service Assessment and Sensitivity Analysis of a Typical Mine–Agriculture–Urban Compound Area in North Shanxi, China. *Land* **2022**, *11*, 1378. [CrossRef]
12. Burtseva, E.; Sleptsov, A.; Bysyina, A.; Fedorova, A.; Dyachkovski, G.; Pavlova, A. Mining industry of the Republic of Sakha (Yakutia) and problems of environmental and social security of indigenous peoples. *Land* **2022**, *11*, 105. [CrossRef]
13. Bhadra, B.; Gupta, A.; Sharma, J.; Choudhary, B. Mining activity and its impact on the environment: Study from Makrana marble and Jodhpur sandstone mining areas of Rajasthan. *J. Geol. Soc. India* **2007**, *70*, 557–570.
14. Li, S.; Zhao, Y.; Xiao, W.; Yue, W.; Wu, T. Optimizing ecological security pattern in the coal resource-based city: A case study in Shuozhou City, China. *Ecol. Indic.* **2021**, *130*, 108026. [CrossRef]
15. Shan, Y.; Dai, X.; Li, W.; Yang, Z.; Wang, Y.; Qu, G.; Liu, W.; Ren, J.; Li, C.; Liang, S. Detecting spatial-temporal changes of urban environment quality by remote sensing-based ecological indices: A case study in Panzhihua city, Sichuan Province, China. *Remote Sens.* **2022**, *14*, 4137. [CrossRef]
16. Tang, Q.; Wang, J.; Jing, Z. Tempo-spatial changes of ecological vulnerability in resource-based urban based on genetic projection pursuit model. *Ecol. Indic.* **2021**, *121*, 107059. [CrossRef]
17. Chormare, R.; Kumar, M.A. Environmental health and risk assessment metrics with special mention to biotransfer, bioaccumulation and biomagnification of environmental pollutants. *Chemosphere* **2022**, *302*, 134836. [CrossRef]
18. Liu, C.; Deng, C.; Li, Z.; Liu, Y.; Wang, S. Optimization of spatial pattern of land use: Progress, frontiers, and prospects. *Int. J. Environ. Res. Public Health* **2022**, *19*, 5805. [CrossRef]
19. Yang, G.; Zhang, Z.-J.; Cao, Y.-G.; Zhuang, Y.-N.; Yang, K.; Bai, Z.-K. Spatial-temporal heterogeneity of landscape ecological risk of large-scale open-pit mining area in north Shanxi. *Chin. J. Ecol.* **2021**, *40*, 187–198. [CrossRef]
20. Li, J.; Sun, W.; Li, M.; Meng, L. Coupling coordination degree of production, living and ecological spaces and its influencing factors in the Yellow River Basin. *J. Clean. Prod.* **2021**, *298*, 126803. [CrossRef]
21. Cui, R.; Han, J.; Hu, Z. Assessment of Spatial Temporal Changes of Ecological Environment Quality: A Case Study in Huaibei City, China. *Land* **2022**, *11*, 944. [CrossRef]
22. Zhang, N.; Xiong, K.; Xiao, H.; Zhang, J.; Shen, C. Ecological Environment Dynamic Monitoring and Driving Force Analysis of Karst World Heritage Sites Based on Remote-Sensing: A Case Study of Shibing Karst. *Land* **2023**, *12*, 184. [CrossRef]
23. Li, Z.; Deng, X.; Jin, G.; Mohmmed, A.; Arowolo, A.O. Tradeoffs between agricultural production and ecosystem services: A case study in Zhangye, Northwest China. *Sci. Total Environ.* **2020**, *707*, 136032. [CrossRef] [PubMed]
24. Huang, S.; Tang, L.; Hupy, J.P.; Wang, Y.; Shao, G. A commentary review on the use of normalized difference vegetation index (NDVI) in the era of popular remote sensing. *J. For. Res.* **2021**, *32*, 1–6. [CrossRef]
25. Du, L.; Song, N.; Liu, K.; Hou, J.; Hu, Y.; Zhu, Y.; Wang, X.; Wang, L.; Guo, Y. Comparison of two simulation methods of the temperature vegetation dryness index (TVDI) for drought monitoring in semi-arid regions of China. *Remote Sens.* **2017**, *9*, 177. [CrossRef]
26. Zhang, S.; Yang, P.; Xia, J.; Qi, K.; Wang, W.; Cai, W.; Chen, N. Research and analysis of ecological environment quality in the Middle Reaches of the Yangtze River Basin between 2000 and 2019. *Remote Sens.* **2021**, *13*, 4475. [CrossRef]

27. Millennium Ecosystem Assessment. *Ecosystems and Human Well-Being: Wetlands and Water*; World Resources Institute: Washington, DC, USA, 2005.
28. Yue, A.; Zhang, Z. Analysis and research on ecological situation change based on EI value. *J. Green Sci. Technol.* **2018**, *14*, 182–184.
29. Geng, J.; Yu, K.; Xie, Z.; Zhao, G.; Ai, J.; Yang, L.; Yang, H.; Liu, J. Analysis of spatiotemporal variation and drivers of ecological quality in Fuzhou based on RSEI. *Remote Sens.* **2022**, *14*, 4900. [CrossRef]
30. Xu, H. A remote sensing urban ecological index and its application. *Acta Ecol. Sin.* **2013**, *33*, 7853–7862.
31. Xu, H.; Wang, M.; Shi, T.; Guan, H.; Fang, C.; Lin, Z. Prediction of ecological effects of potential population and impervious surface increases using a remote sensing based ecological index (RSEI). *Ecol. Indic.* **2018**, *93*, 730–740. [CrossRef]
32. Zhu, D.; Chen, T.; Zhen, N.; Niu, R. Monitoring the effects of open-pit mining on the eco-environment using a moving window-based remote sensing ecological index. *Environ. Sci. Pollut. Res.* **2020**, *27*, 15716–15728. [CrossRef] [PubMed]
33. Tao, Z.; Hong, T. Vegetation cover change and urban expansion in Beijing-Tianjin-Hebei during 2001~2015 based on Google Earth Engine. *Remote Sens. Technol. Appl.* **2018**, *33*, 593–599.
34. Xiong, Y.; Xu, W.; Lu, N.; Huang, S.; Wu, C.; Wang, L.; Dai, F.; Kou, W. Assessment of spatial–temporal changes of ecological environment quality based on RSEI and GEE: A case study in Erhai Lake Basin, Yunnan province, China. *Ecol. Indic.* **2021**, *125*, 107518. [CrossRef]
35. Nie, X.; Hu, Z.; Zhu, Q.; Ruan, M. Research on temporal and spatial resolution and the driving forces of ecological environment quality in coal mining areas considering topographic correction. *Remote Sens.* **2021**, *13*, 2815. [CrossRef]
36. Yuan, B.; Fu, L.; Zou, Y.; Zhang, S.; Chen, X.; Li, F.; Deng, Z.; Xie, Y. Spatiotemporal change detection of ecological quality and the associated affecting factors in Dongting Lake Basin, based on RSEI. *J. Clean. Prod.* **2021**, *302*, 126995. [CrossRef]
37. Liu, C.; Yang, M.; Hou, Y.; Zhao, Y.; Xue, X. Spatiotemporal evolution of island ecological quality under different urban densities: A comparative analysis of Xiamen and Kinmen Islands, southeast China. *Ecol. Indic.* **2021**, *124*, 107438. [CrossRef]
38. Zhang, J.; Zhou, Q.; Cao, M.; Liu, H. Spatiotemporal Change of Eco-Environmental Quality in the Oasis City and Its Correlation with Urbanization Based on RSEI: A Case Study of Urumqi, China. *Sustainability* **2022**, *14*, 9227. [CrossRef]
39. Firozjaei, M.K.; Sedighi, A.; Firozjaei, H.K.; Kiavarz, M.; Homaee, M.; Arsanjani, J.J.; Makki, M.; Naimi, B.; Alavipanah, S.K. A historical and future impact assessment of mining activities on surface biophysical characteristics change: A remote sensing-based approach. *Ecol. Indic.* **2021**, *122*, 107264. [CrossRef]
40. Lin, L.; Hao, Z.; Post, C.J.; Mikhailova, E.A. Monitoring Ecological Changes on a Rapidly Urbanizing Island Using a Remote Sensing-Based Ecological Index Produced Time Series. *Remote Sens.* **2022**, *14*, 5773. [CrossRef]
41. Yu, G.; Liu, T.; Wang, Q.; Li, T.; Li, X.; Song, G.; Feng, Y. Impact of Land Use/Land Cover Change on Ecological Quality during Urbanization in the Lower Yellow River Basin: A Case Study of Jinan City. *Remote Sens.* **2022**, *14*, 6273. [CrossRef]
42. Shan, W.; Jin, X.; Ren, J.; Wang, Y.; Xu, Z.; Fan, Y.; Gu, Z.; Hong, C.; Lin, J.; Zhou, Y. Ecological environment quality assessment based on remote sensing data for land consolidation. *J. Clean. Prod.* **2019**, *239*, 118126. [CrossRef]
43. Zhang, X.; Yang, L.; Li, Y.; Li, H.; Wang, W.; Ye, B. Impacts of lead/zinc mining and smelting on the environment and human health in China. *Environ. Monit. Assess.* **2012**, *184*, 2261–2273. [CrossRef] [PubMed]
44. Tang, H.; Fang, J.; Xie, R.; Ji, X.; Li, D.; Yuan, J. Impact of Land Cover Change on a Typical Mining Region and Its Ecological Environment Quality Evaluation Using Remote Sensing Based Ecological Index (RSEI). *Sustainability* **2022**, *14*, 12694. [CrossRef]
45. Zhao, W.; Yan, T.; Ding, X.; Peng, S.; Chen, H.; Fu, Y.; Zhou, Z. Response of ecological quality to the evolution of land use structure in Taiyuan during 2003 to 2018. *Alex. Eng. J.* **2021**, *60*, 1777–1785. [CrossRef]
46. da Cunha, E.R.; Santos, C.A.G.; da Silva, R.M.; Bacani, V.M.; Pott, A. Future scenarios based on a CA-Markov land use and land cover simulation model for a tropical humid basin in the Cerrado/Atlantic forest ecotone of Brazil. *Land Use Policy* **2021**, *101*, 105141. [CrossRef]
47. Lambin, E.F.; Geist, H.J.; Lepers, E. Dynamics of land-use and land-cover change in tropical regions. *Annu. Rev. Environ. Resour.* **2003**, *28*, 205–241. [CrossRef]
48. Sun, D.; Kafatos, M. Note on the NDVI-LST relationship and the use of temperature-related drought indices over North America. *Geophys. Res. Lett.* **2007**, *34*. [CrossRef]
49. Wu, Z.; Lei, S.; Lu, Q.; Bian, Z.; Ge, S. Spatial distribution of the impact of surface mining on the landscape ecological health of semi-arid grasslands. *Ecol. Indic.* **2020**, *111*, 105996. [CrossRef]
50. Hu, X.; Xu, H. A new remote sensing index for assessing the spatial heterogeneity in urban ecological quality: A case from Fuzhou City, China. *Ecol. Indic.* **2018**, *89*, 11–21. [CrossRef]
51. Yue, H.; Liu, Y.; Li, Y.; Lu, Y. Eco-environmental quality assessment in China's 35 major cities based on remote sensing ecological index. *IEEE Access* **2019**, *7*, 51295–51311. [CrossRef]
52. Wu, Y.; Li, S.; Yu, S. Monitoring urban expansion and its effects on land use and land cover changes in Guangzhou city, China. *Environ. Monit. Assess.* **2016**, *188*, 54. [CrossRef]
53. Kamga, M.A.; Nguemhe Fils, S.C.; Ayodele, M.O.; Olatubara, C.O.; Nzali, S.; Adenikinju, A.; Khalifa, M. Evaluation of land use/land cover changes due to gold mining activities from 1987 to 2017 using landsat imagery, East Cameroon. *GeoJournal* **2020**, *85*, 1097–1114. [CrossRef]
54. Ding, Y.; Peng, J. Impacts of urbanization of mountainous areas on resources and environment: Based on ecological footprint model. *Sustainability* **2018**, *10*, 765. [CrossRef]

55. Zhang, H.C.G.; Wang, B.; Jiang, X. 6 Urban master planning in China: A case study of policy and practice in Hua County. In *The Routledge Handbook of Planning Research Methods*; Routledge: New York, NY, USA, 2014; pp. 491–506.
56. Zhou, K.; Wang, X.; Wang, Z.; Hu, Y. Systematicity and Stability Analysis of Land Use Change—Taking Jinan, China, as an Example. *Land* **2022**, *11*, 1045. [CrossRef]
57. Wang, J.; Wang, W.; Zhang, S.; Wang, Y.; Sun, Z.; Wu, B. Spatial and temporal changes and development predictions of urban green spaces in Jinan City, Shandong, China. *Ecol. Indic.* **2023**, *152*, 110373. [CrossRef]
58. Bhargava, A.; Lakmini, S.; Bhargava, S. Urban Heat Island Effect: It's relevance in urban planning. *J. Biodivers. Endanger. Species* **2017**, *5*, 2020.
59. Liu, P.; Hu, Y.; Jia, W. Land use optimization research based on FLUS model and ecosystem services–setting Jinan City as an example. *Urban Clim.* **2021**, *40*, 100984. [CrossRef]
60. Lei, K.; Pan, H.; Lin, C. A landscape approach towards ecological restoration and sustainable development of mining areas. *Ecol. Eng.* **2016**, *90*, 320–325. [CrossRef]
61. Zhou, J.; Liu, W. Monitoring and evaluation of eco-environment quality based on remote sensing-based ecological index (RSEI) in Taihu Lake Basin, China. *Sustainability* **2022**, *14*, 5642. [CrossRef]
62. Yuan, Y.; Bai, Z.; Zhang, J.; Xu, C. Increasing urban ecological resilience based on ecological security pattern: A case study in a resource-based city. *Ecol. Eng.* **2022**, *175*, 106486. [CrossRef]